J. Cell. Mol. Med. Vol 13, No 7, 2009 pp. 1321-1335

Apoptosis-related mitochondrial dysfunction defines human monocyte-derived dendritic cells with impaired immuno-stimulatory capacities

Laurent Castera [a, ‡], Anne Sophie Hatzfeld-Charbonnier [a, ‡], Caroline Ballot [a], Florence Charbonnel [a], Edith Dhuiege [a], Thierry Velu [b], Pierre Formstecher [a], Laurent Mortier [a, †], Philippe Marchetti [a, *, †]

[a] Inserm U837 and Plate-forme de Biothérapie, Faculté de Médecine Université de Lille II 1, Place Verdun Lille Cedex France et Centre de Biologie Pathologie CHRU Lille, France
[b] Department of Medical Oncology, Erasme Hospital, Université Libre de Bruxelles, Route de Lennik, Brussels, Belgium

Received: December 7, 2007; Accepted: April 21, 2008

Abstract

The death of dendritic cells (DCs) can potentially influence immune responses by affecting the duration of DC stimulation of lymphocytes. Here, we report that cultured mature monocyte-derived DCs manifest early mitochondrial damage (*i.e.* within 24 hrs), characterized by mitochondrial membrane potential ($\psi\Delta m$) disruption and mitochondrial release of pro-apoptotic factors, followed by reactive oxygen species (ROS) production and activation of caspases. Afterwards, DCs with mitochondrial alterations are condemned to undergo apoptosis and necrosis. Macroarray analysis results (validated by real time quantitative-PCR (QRT-PCR) and immunoblotting), showed up-regulation of the pro-apoptotic member of the Bcl-2 family, Bim, while expression of several anti-apoptotic molecules was down-regulated. Importantly, pre-apoptotic DCs (characterized by a low $\Delta\psi m$) showed a modified phenotype, with down-regulation.of HLA-DR and of the co-stimulatory molecules CD80 and CD86. Moreover, sorted viable low $\psi\Delta m$ DCs were unable to activate allogeneic T cells, indicating that pre-apoptotic DCs have already lost some of their immuno-stimulatory capabilities long before any detectable signs of death occur. Perturbations to mitochondrial respiration with rotenone identified the same modifications to DC immune functions. These data indicate a strong requirement for mitochondrial integrity for the immuno-stimulatory capacities of DC. Determining $\Delta\Psi m$ could be a useful parameter to select 'fully' functional DCs for anti-tumour vaccines.

Keywords: apoptosis • DC longevity • immunotherapy

Introduction

A delicate balance between cell death by apoptosis and cell survival is a key mechanism for proper regulation of the immune system. Apoptosis has to take place constantly to counterbalance immune cell activation and proliferation. Hence, lymphocyte apoptosis is at the heart of the homeostatic regulation of the immune system. However, lessons from animal models indicate that death of other immune cell types may also be critical for the maintenance of correct immune responses. As dendritic cells (DCs) are the main antigen presenting cells, with an unequalled capacity for eliciting immune responses, the control of their number and lifespan might also influence the regulation of the immune system. Consequently, much attention has been paid recently to the role of DC apoptosis in the maintenance of proper immune control. In mice, spontaneous death in DCs regulates the immune response [1]. As a result, DCs with an increased lifespan induce a stronger immune response [1–3]. In transgenic mice selectively expressing apoptosis inhibitors in their DCs, defective DC apoptosis leads to DC accumulation which, in turn, induces lymphocyte over-activation, resulting in the onset of systemic autoimmunity [4]. Conversely,

† P.M. and L.M. share the co-seniorship of this paper.
‡ L.C. and A.S.H.C. contributed equally to this paper.
*Correspondence to: Philippe MARCHETTI, M.D., Ph.D.,
Inserm U 837, 1 Place Verdun, F- 59045 Lille Cedex, France
Tel.: +00-33-3-20-62-69-52
Fax: +00-33-3-20-62-68-84
E-mail: philippe.marchetti@lille.inserm.fr

doi:10.1111/j.1582-4934.2008.00358.x

one can imagine that accelerated clearance of DCs by apoptosis reduces their duration for stimulating lymphocytes, thereby, leading to a less effective immune response.

Nuclear alterations accompanying apoptosis are late events of the apoptotic cascade and occur under the control of two canonical apoptosis pathways. The extrinsic apoptosis pathway is mediated by death receptors, such as the receptors for Fas and tumour necrosis factor (TNF)-related apoptosis-inducing ligand (TRAIL), and caspase-8, *i.e.* the major initiator caspase in this pathway. Several death receptors, including Fas, are expressed in monocyte-derived DCs. However, DCs are known to be resistant to Fas-induced cell death through the constitutive expression of FLICE (caspase-8)-like inhibitory protein (FLIP), a strong inhibitor of apoptosis initiated by death receptors [5].

The intrinsic apoptosis pathway requires mitochondrial-specific signalling. Mitochondria initiate apoptosis through mitochondrial outer membrane permeabilization and the release of apoptogenic factors (*e.g.* cytochrome c, AIF or Smac/Diablo) from the mitochondrial intermembrane space, leading to cell death through caspase-dependent and -independent pathways. Signalling cascades can also affect the inner mitochondrial membrane permeability in apoptosis and necrosis. As a consequence, cells also exhibit a loss of electrical potential across the inner membrane which is quantifiable by means of potentiometric dyes, a measure that precedes signs of nuclear apoptosis and cell death [6]. Mitochondrial dysfunction, characterized by marked reduction in mitochondrial membrane potential ($\Delta\psi m$), is an early step of ongoing DC death that can be triggered by many cytotoxic stimuli [7–13]. Inner and outer mitochondrial membrane permeabilization is tightly regulated by the opposing actions of pro- and anti-apoptotic Bcl-2 family members. Compelling evidence indicates that mitochondria-related proteins of the Bcl-2 family are crucial DC death sensors [9, 12, 14–16], substantiating the importance of mitochondria in DC apoptosis.

Owing to their critical role in the induction of antigen-specific T-cell responses, DCs are increasingly used in active immunotherapy of malignant diseases. Currently, much effort is being applied to engineering DCs for active vaccines, which appears to be a promising approach for the development of anti-tumour immune responses. The most frequently described method for obtaining DCs is their *ex vivo* generation from peripheral blood cells, such as monocytes. Generally, these monocyte-derived DCs are subjected to a process of maturation prior to their administration to patients. Several reports recently advocated that the immunostimulatory properties of DC-based vaccines are limited by their short lifespan [16, 17]. In this context, unveiling the mechanisms regulating mature monocyte-derived DC death is fundamental for developing a better understanding of their effects on immune functions. Therefore, we examined the mechanisms of spontaneous apoptosis of DCs by focusing on an early event, mitochondrial dysfunction, and clarified the consequences of commitment to apoptosis on DC immuno-stimulatory functions. Rapid commitment of DCs to apoptosis was associated with impaired capacity to induce an immune response long before the loss of DC viability. These insights are important for further understanding DC depletion, as well as for the direct quantitative evaluation of ongoing apoptosis in clinically used DCs. We propose that mitochondrial alterations in DCs should be considered, and exploited, for anti-tumour vaccine development.

Materials and methods

Reagents

Lipopolysaccharide from *Escherichia coli* serotype 0111:B4 (LPS), propidium iodide (PI), rotenone and carbamoyl cyanide m-chlorophenylhydrazone (mClCCP) were obtained from Sigma (Lyon, France). GMCSF and IL4 were from ProSpec-Tany Techno Gene Ltd. (Le Perray en Yvelines, France). The 5-(and-6)-carboxyfluorescein diacetate, succinimidyl ester (CFSE) was from Invitrogen (Cergy Pontoise, France). Z-VAD-fmk was from Bachem (Budendorf, Switzerland). The 3,3′-dihexyloxacarbocyanine iodide (DiOC6(3)), hydroethidine (HE), chloromethyl-X-Rosamine (CMX-ROS) were purchased from Molecular Probes Inc. (Eugene, OR, USA). FITC-VAD-fmk was from Promega (Madison, WI, USA).

DC generation

DCs were generated from monocytes issued from buffy coats taken from healthy donors, as previously described [18]. For maturation, DCs were then cultured with 1μg/ml LPS for 18 hrs in the presence of GMCSF (800 U/ml) and IL4 (100 U/ml) in six-well plates at 10^6 cells/ml. Alternatively, DCs were subjected to maturation with 10 μg/ml poly (I:C) (Sigma) or 5 μg/ml anti-CD40 mAb (Diaclone, Besançon, France). Afterwards, mature DCs were washed, analysed or further cultured for 4 days in complete RPMI.

Detection of cell death

Assessment of PS exposure was performed by the binding of annexin V-FITC, using the protocol outlined in the FITC-Annexin kit (BD Pharmingen, Le Pont de Claix, France). The frequency of hypoploid cells (sub-G1 cells) was assessed, as described previously [19]. DNA fragmentation (10×10^6 cells/lane) was determined by horizontal agarose gel electrophoresis, following published methods [19]. Measurement of the specific activity of caspases was performed with Caspase-Glo 3/7, Caspase-Glo 8 and Caspase-Glo 9 assay kits (Promega) following the manufacturers' instructions.

Cytofluorometric assessment of $\Delta\Psi m$ and ROS production

$\Delta\Psi m$ was measured by means of DiOC6(3) or CMX-ROS, as described [20]. Pilot experiments indicated that both fluorochromes were reliable probes to monitor $\Delta\psi m$ in DCs (not shown) and so the choice of fluorochrome used depended on its fluorescence spectrum in order to permit its use in combination with other fluorescent dyes. DiOC6(3) produces a single fluorescent emission peak collected through the FL1 detector

(525+- 5 nm band pass filter allowing combination with the supravital fluorochrome PI (5 μg/ml in PBS just before analysis) or with HE (1 μM in PBS, 15 min. at 37°C) to measure ROS production, both of which emitted fluorescence signals detected through the FL3 detector (620 ± 5 nm band pass filter). Samples were stored on ice before cytofluorometric analysis. Control experiments were done in the presence of 10 μmol/l mClCCP, an uncoupling agent that abolishes $\Delta\psi m$, for 15 min. at 37°C. For all cytofluorometric experiments, a minimum of 10,000 cells were analysed on a Coulter XL cytometer (Beckman-Coulter, Villepinte, France). Assessment of DC viability and $\Delta\psi m$ simultaneously allowed sorting of the viable population of DC in relation to their $\Delta\psi m$ [21]. Immediately after staining, DCs were sorted flow cytometrically on a Coulter ALTRA cell sorter. The standard mode 'ultimate purity' was used to sort DCs with high purity. The sorter was operated at 10 psi with sheath fluid. Sort gates were placed around viable (PI or YOPRO negative cells), $\Delta\psi m$ high or $\Delta\psi m$ low DC populations. The purity of sorted cell populations was checked by immediate re-analysis and was always >98%.

Mitochondrial calcium retention capacity

For determination of mitochondrial calcium loading, a procedure described previously [22] was used with some modifications. At the times indicated, 2×10^6 DCs were suspended in 1 ml of buffer (150 mM KCl, 5 mM KH2PO4, 1 mM MgCl2, 5 mM succinate, 5 mM Tris, pH 7.4) and permeabilized with 0.002% digitonin. Calcium concentration changes were continuously recorded in a multi-port measurement chamber (NOCHM-4, WPI, Aston, UK) equipped with calcium-sensitive and reference electrodes. At the end of the incubation period, 10 μM $CaCl_2$ pulses were performed with a micro-syringe injector adapted to a Micro4 pump controller (UMPII and Micro-4, WPI).

Immunofluorescence microscopy

Sub-cellular distribution of AIF and cyt c was revealed by immunofluorescence staining and nuclei counterstained with Hoeschst 33342 following published methods [19].

Cell surface immunostaining

All FITC-conjugated mAbs used were purchased from Becton Dickinson, (Le Pont de Claix, France). FITC-conjugated antimouse IgG was from Jackson Immunoresearch (West Baltimore, MD, USA). For the simultaneous assessment of surface markers and $\Delta\psi m$, DCs were first stained with 50 nM CMX-ROS at room temperature for 30 min. (fluorescence was collected through the FL3 detector) and then stained with appropriate dilutions of FITC-conjugated anti-CD1a, anti-HLA-DR, anti-CD86, anti-CD80, anti-CD11c or anti-CD83 antibodies for 30 min. on ice prior to flow cytometric analysis.

Allogenic naïve T-cell response

T-cell activation was assessed by flow cytometry measuring CFSE fluorescence intensity as described previously [18]. Second, IFN-γ, IL-4 and IL-10 production by T cells co-cultured with DCs was measured in day 5 co-culture supernatants by ELISA (Diaclone).

Apoptosis gene superarray

DCs were collected immediately after maturation (D0) or cultured for 24 hrs in complete RPMI as above (D1). After removing the supernatant, total RNA was extracted using the Qiagen RNeasy mini Kit Qiagen SA (Courtaboeuf, France). RNA samples were checked for quality using a 2100 Bioanalyzer (Agilent Technologies, Palo Alto, CA, USA). Samples were frozen at –80°C until use in superarray. For analysis, 3 μg of RNA was reverse-transcribed with Biotin-16-dUTP (Roche Diagnostics, Meylan, France) using a SuperArray TrueLabeling-RT Enzyme kit (SuperArray, Inc., Frederick, MD, USA) according to the manufacturer's instructions. The resulting biotinylated cDNA probe mixture was allowed to hybridize overnight to the Q Series Human Apoptosis (Cat no: HS-002, SuperArray, Inc. [see www.superarray.com for detail]) at 60°C overnight. Data were acquired and analysed according to the manufacturer's protocol. All signal intensities were PUC18 plasmid DNA (negative control) background subtracted and normalized to cyclophilin A spots (positive control). Scatter plots were made from normalized signals. The relative expression level of each gene was based on the ratio of cyclophilin A. Changes in gene expression were illustrated as a fold increase/decrease. Experiments were repeated three times.

Real-time quantitative reverse transcriptase-polymerase chain reaction

The PCR was carried out with the LC FastStart Masterplus SYBR green I kit (Roche Applied Science, Mannheim, Germany) using 200 ng of cDNA in a 10 μl final volume, 0.5 μM of each primer (final concentration). Primers used for qPCR were: CFLAR (sense) 5′-GTGTGGATCAGACTCACTCAGGG-3′, (forwards) 5′-CATAGTTCTGA-ATAAAAAACATCTTTGGC-3′, MCL1 (sense) 5′-GCAGC-GCAACC ACGAGA-3′ (forwards) 5′-CTAATGGTTCGATG-CAGCTTTCT-3′, BCL2L1 (sense) 5′-CATGGCAGCAGTA-AAGCAAG-3′(forwards) 5′-ACAATGCGACCCCAGTTT-AC-3′, BCL2L11 (sense) 5′-AAGACAGGAGCCCAGCA-CC-3′ (forwards) 5′-TCTTCGGCTGCTTGGTAATTATTC-3′, RIPK2 (sense) 5′-AACGTCTGCAGCCTGGTATAGC-3′ (forwards) 5′-TTGAGGTCCTTGTAGGCTTGGTA-3′, TNFRSF6 (sense) 5′-TCTTTCTCAGGCATCAAAAGCAT-3′ (forwards) 5′-TGGAGAGGTGGCAAAGCTCTA-3′, GADD45A (sense) 5′-TGCGAGAACGACATCAACAT-3′ (forwards) 5′-TGATCCATGTAGCGACTTTC-3′, TNFSF10 (sense) 5′-CTGTG TGGCTGTAACTTACGTGTACTT-3′ (forwards) 5′-TTCTAACGAGCTGACGGAGTTG-3′, CHEK1 (sense) 5′-AGAATAGAGCCAGACATAGG-3′ (forwards) 5′-TCTTCAG AAGTTCTGGAGCA-3′, 18S F-TCCCAGTAAGTGCGGGTCA-3′ (forwards) 5′-GATCCGAGGGCCTCACTAAAC-3′. Quantitative PCR was performed with a Lightcycler (Roche Applied Science). The cycling protocol consists of pre-incubation at 95°C for 10 min., followed by 40 cycles of denaturation at 95°C for 10 sec., annealing at 60°C for 20 sec. and extension at 72°C for 25 sec. Fluorescence was measured at the end of each extension phase. Immediately after amplification, melting curve data analysis (for dimer primer detection) was performed by measuring the fluorescent signal during the following cycling profile: 95°C for 0 sec., 65°C for 15 sec., 95°C for 0 sec. and 40°C for 30 sec. For each sample, the average crossing-point value (number of cycles at which each sample reached a threshold fluorescence value) was calculated from triplicate reactions and is indicated as cycle threshold (Ct). Expression of apoptotic genes are calculated relative to 18s mRNA levels by the comparative ΔCt method. Ct value for the apoptotic genes and for 18S was measured. The relative transcript levels were calculated as $x = 2^{-\Delta Ct}$, in which $\Delta Ct = Ct_{gene} - Ct_{18s}$. Each Ct value was determined from three parallel real-time PCRs.

Immunoblotting

To obtain whole-cell lysates, Laemmli's loading buffer (100 µl/10^6 cells) was added to harvested cells and samples were boiled for 5 min. Alternatively, the cytosolic protein fraction was obtained according to procedures previously described [19]. The release of mitochondrial proteins has been tested on cytosolic protein fractions whereas other immunoblotting were performed on whole-cell lysates. For all, 50 µg of protein was loaded onto 12% polyacrylamide gels, electrophoresed, transferred and detected as previously described [19]. Membranes were incubated with one of the following primary antibodies overnight at 4°C: either anti-cytochrome c (1:1000, clone 7H8.2C12, Pharmingen), anti-AIF (1:1000, sc-13116, Santa Cruz Biotechnology Inc., Santa Cruz, CA, USA), anti-Bcl-X (1:1000,clone L-19, Santa Cruz Biotechnology Inc.), anti-Bcl-2 (1:1000, clone 100, Santa Cruz Biotechnology Inc.), anti-FLIP (1:1000, clone H-202, Santa Cruz Biotechnology Inc.), anti-Bim (1:1000, clone H-191, Santa Cruz Biotechnology Inc.), anti-Bax (1:1000,clone N-20, Santa Cruz Biotechnology Inc.), anti-Bad (1:1000, clone H-168, Santa Cruz Biotechnology Inc.), anti-Smac/Diablo (1:500 from Calbiochem (San Diego, USA)), anti-caspase 3 (1:250 from Cell Signaling [Saint Quentin en Yvelines, France]), anti-XIAP (1:1000 from Stressgen [Michigan, Germany]), or anti-cytochrome c oxidase (subunit IV 1:500 from Molecular Probes Inc.). Membranes were stripped and re-probed with anti-actin or anti G3PDH antibodies (1:1000 from Sigma) to check for equal loading.

Statistical analysis

Data were analysed using GraphPad Prism version 3.00 (GraphPad Software, San Diego, CA, USA). For comparison of two subgroups of DCs ($\Delta\psi m$ high DCs *versus* $\Delta\psi m$ low DCs), a two-tailed Wilcoxon rank test was employed. Values of $P < 0.05$ were considered statistically significant. Kolmogorovi-Smirnov statistical analysis of flow cytometric data were used according to Expo 32 software (Beckman-Coulter).

Results

Characteristics of spontaneous DC death in culture

The levels of spontaneous cell death in monocyte-derived DCs were first determined. We cultured freshly matured human monocyte-derived DCs for up to 4 days in complete medium (RPMI including 10% foetal calf serum) and every day an aliquot of cells was examined by dual staining flow cytometry with annexin V and the vital dye PI. Annexin V-positive and PI-negative cells were identified as apoptotic DCs and cells that were both PI-positive and annexin V-positive identified as dead DCs (secondary necrosis) (Fig. 1A). The number of apoptotic DCs increased during the first days of culture (up to 2 days). This was followed by a plateau phase, although the number of dead cells then steadily increased, and after 4 days of culture approximately 50% of DCs were dead (Fig. 1A). Kinetic studies of sub-G1 cells and PI uptake, respectively, indicated that the apoptotic percentage was lower than the percentage of dead (PI-positive) cells (Fig. 1B), confirming the results obtained with annexin V/PI (Fig. 1A). Additionally, the microscopic images of cells stained with MGG demonstrated the significant presence of apoptotic DCs (*i.e.* condensed nuclei and shrunken cytoplasm) occurring after 2 days of culture (Fig. 1C). This observation of apoptotic cells was confirmed by the presence of the electophoretic pattern of DNA laddering (Fig. 1D). Contrasting with the presence of apoptotic features, cellular signs of primary necrosis, such as cells with loose nuclei and swollen cytoplasm, were found in 10–20% of DCs in association with cell debris later, *i.e.* at day 4 of culture (Fig. 1C). Thus, freshly matured monocyte-derived DCs underwent constitutive cell death characterized by hallmarks of apoptosis, as well as necrosis.

Apoptotic pathways involved in spontaneous DC death

To further explore the mechanism of constitutive apoptosis in DCs, we sought to investigate the role of effector caspases as well as mitochondria, two main contributors to classical apoptosis. As previously reported [23], we observed significant caspase-3/-7-like activity as early as day 0, and which increased twofold after 1 day of culture (Fig. 2A, left part) *i.e.* before the appearance of nuclear apoptosis (Fig. 1). This increase was maintained for up to 4 days of culture. This profile was accompanied by enhancement of the proteolytic activation of caspase-3 (Fig. 2A, right part). The mitochondrion is a key regulator that

controls cell life and death by releasing several death-promoting factors into the cytosol [24]. To examine the involvement of mitochondria in DC death, cytosolic extracts were prepared at various times from DCs in culture and subjected to immunoblotting. The immunoblotting results indicated that the pro-mitochondrial factors cytochrome c, AIF and Smac/Diablo were substantially raised in cytosolic fractions at day 1 of culture (Fig. 2B). Sub-cellular distribution of cyt c and AIF was also monitored by immunofluorescence microcopy confirming the spontaneous release of proapoptotic proteins (Fig. 2B). The cytosolic accumulation of cytochrome c and AIF was not abrogated by z-VAD.fmk (Fig. 2B) at concentrations that completely block caspase activity (Fig. 2A), suggesting that caspases must act downstream of the mitochondrial signals. However, it is to note that cytosolic accumulation of Smac/Diablo was slightly attenuated in z-VAD.fmk treated cells, a result previously observed in other cell types [25].

In many models of apoptosis, the release of mitochondrial pro-apoptotic factors is accompanied by a step-wise dysregulation of mitochondrial functions. This mitochondrial dysfunction is characterized by a loss of $\Delta\psi m$, followed by the subsequent generation of ROS resulting from uncoupling of the respiratory chain [26]. We performed a kinetic analysis of the appearance of these mitochondrial alterations in cultured DCs (Fig. 2C). At the times indicated, an aliquot of DCs was stained with the potential-sensitive dye DiOC6(3) and with the ROS reactive compound HE (Fig. 2C). As shown in Fig. 2C, disruption of $\Delta\psi m$ measured by the reduc-

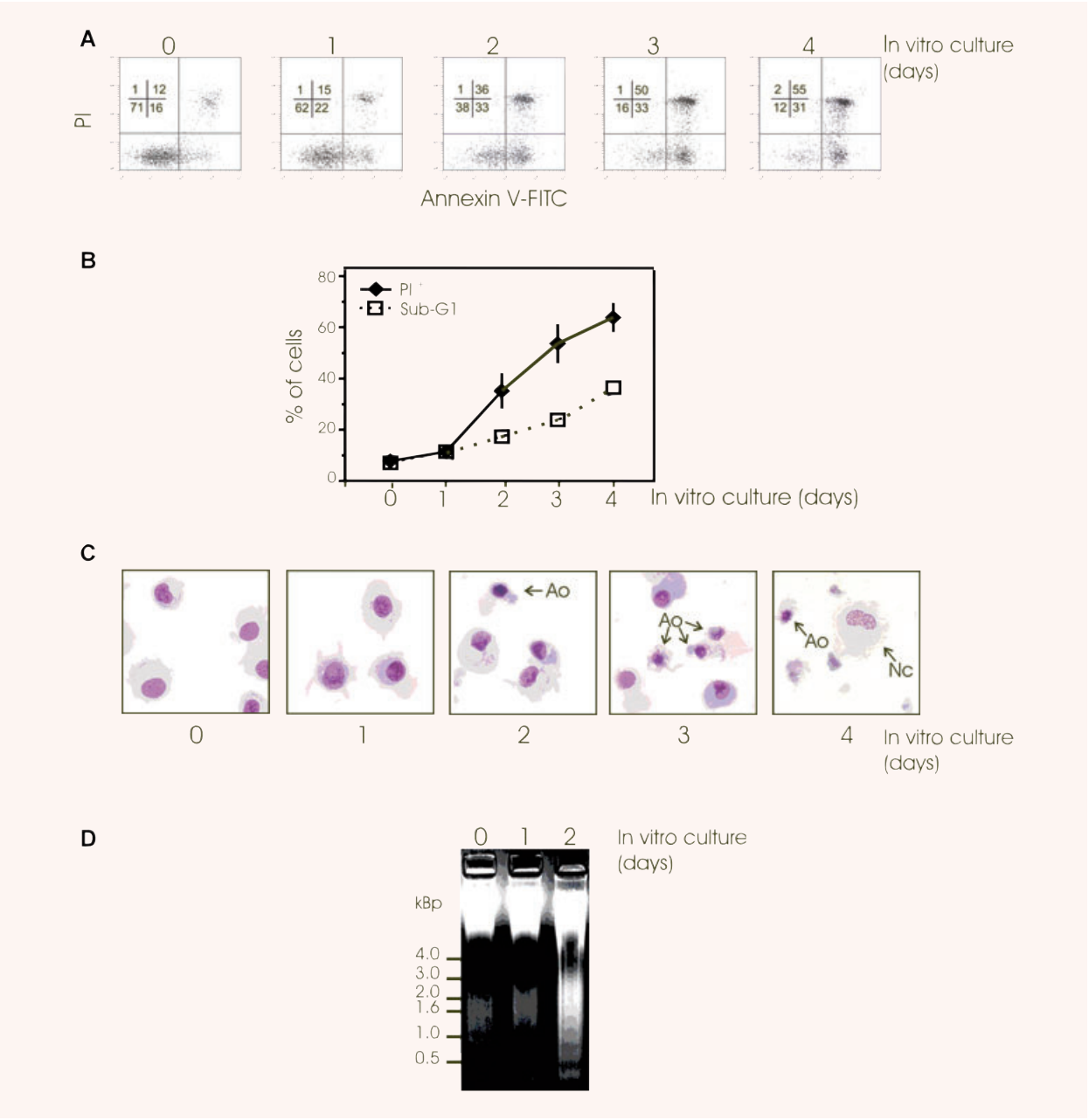

Fig. 1 Spontaneous death of freshly matured human monocyte-derived DCs. Immediately after maturation, human monocyte-derived DCs were cultured under standard conditions for 4 days and an aliquot of cells was collected every day for cell death determination (0, 1, 2, 3 or 4 days of culture). (**A**) Flow cytometric analysis of Annexin V-FITC binding and PI staining in cultured DCs at different incubation times (days). The percentage of DCs in each quadrant is indicated. Similar results were obtained from five separate donors. (**B**) Flow cytometric determination of the percentage of sub-G1 cells obtained by cell cycle evaluation and the percentage of PI permeable cells (PI +) at different culture intervals (days) is shown. Mean ± S.D. from 5 independent experiments are shown. (**C**) When indicated, cytospin preparations of DCs were stained with May-Grundwald-Giemsa to evaluate general DC morphology (Ao: Apoptotic cell; Nc: Necrotic cell). Micrographs were taken under a transmission electron microscope (original magnification ×630). Two independent experiments gave similar results. (**D**) Agarose gel electrophoresis of DC DNA before (0) and after (1 or 2 days) culture. Two independent experiments gave similar results.

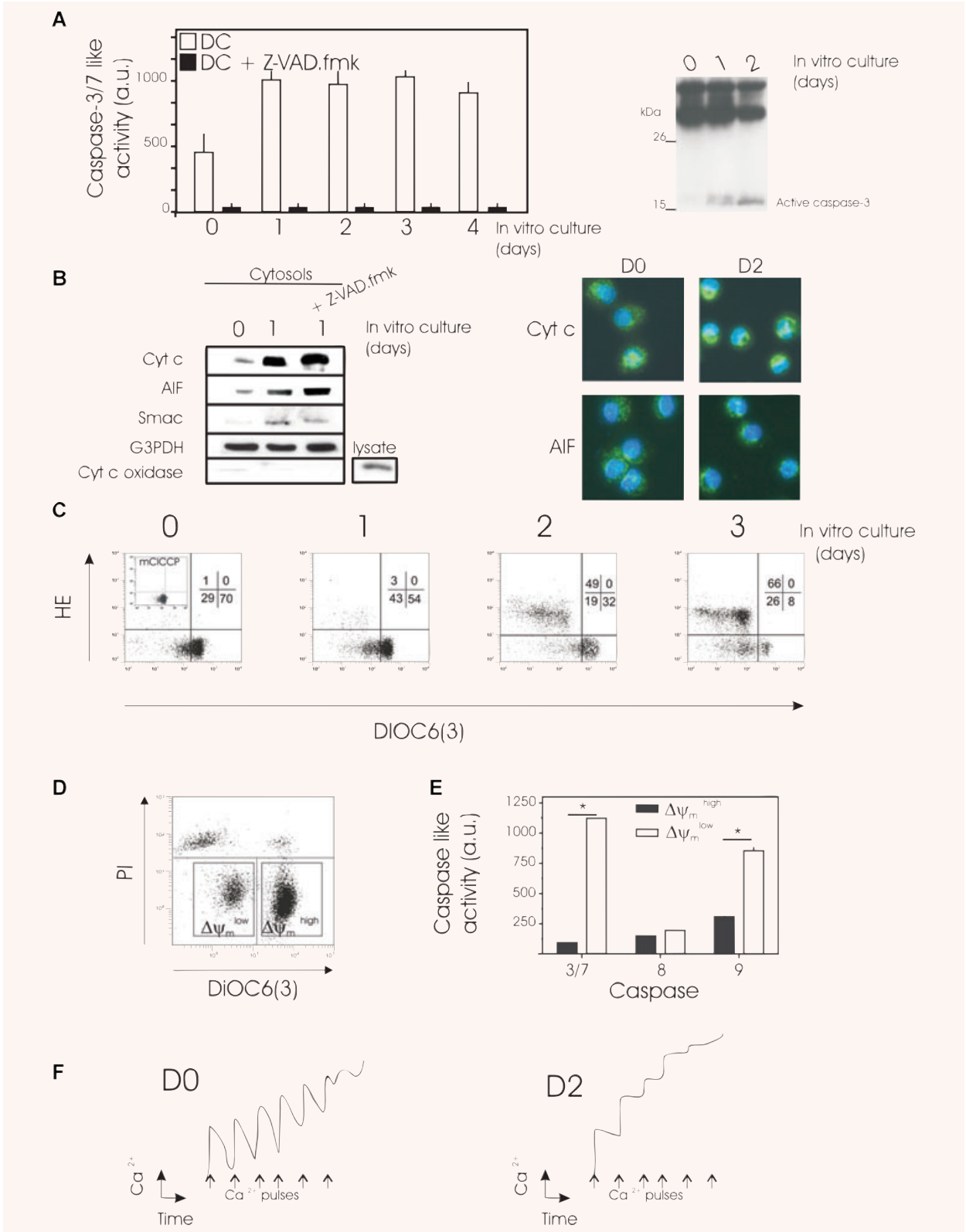

Fig. 2 Spontaneous DC death involves caspase activation and mitochondrial dysfunction. Immediately after maturation, human monocyte-derived DCs were cultured under standard conditions for 4 days and an aliquot of cells was collected every day (0, 1, 2, 3 or 4 days of culture) for determination of caspase activation (**A**) and mitochondrial dysfunction (**B**, **C**, **D**). (**A**) Caspases 3/7 activity was measured (left part) as described in Materials and Methods. When indicated, DCs were exposed for 1 hr to z-VAD-fmk (100 μM) as a positive control for caspase inhibition. Mean ± S.D. from three independent experiments are shown. Active caspase 3 was identified by Western blotting (right part). Three independent experiments gave similar results. (**B**) Cytosolic protein fractions were obtained and cytochrome C, AIF and Smac Diablo mitochondrial release in DCs was evaluated by Western blotting. (left part). When indicated, DCs were treated for 24 hrs with z-VAD-fmk (100 μM). Equal loading was checked by probing with anti-G3PDH antibody. Blots were also probed for cyt c oxidase to exlude mitochondria contamination in the cytosol. As a control for detection of cyt c oxidase, a total lysate was loaded. Fluorescence images (right part) of immunostaining with cytochrome c (green) or AIF (green) and nuclear Hoechst 33342 staining (blue) of DCs at day 0 (D0) or day 1 (D1) of culture. Original magnification ×630. (**C**) Simultaneous assessment of $\Delta\psi$m and ROS production performed with DiOC6(3) and HE. As a control, DCs were incubated with the protonophore mClCCP (100 μM, 15 min., 37°C) as a negative control for DiOC6(3) staining. One representative experiment of four is shown. (**D** and **E**). Mature DCs were cultured for 36 hrs under standard conditions, and cells then stained with DiOC6(3) and PI before flow cytometric analysis. Same results were obtained with CMX-ROS and YOPRO-1 staining. These flow cytometric parameters were used for sorting (**D**). The left square depicts the viable sorted $\Delta\psi$m low subpopulation and the right square represents the $\Delta\Psi$m high counterparts. (**E**) Determination of caspase activity in $\Delta\psi$m-sorted populations as shown in D. Caspases -3/7, -8, and -9 activity was estimated after short-term culture of sorted viable $\Delta\psi$m high and low DC subpopulations (**E**). Mean ± S.D. from three independent experiments are shown. *Statistically significant between purified $\Delta\psi$m low and $\Delta\psi$m high subpopulations. (**F**) Mitochondrial calcium retention capacity. At day 0 (D0, left panel) or day 2 (D2, right panel) of culture, DCs were permeabilized with digitonin and calcium uptake measured with a calcium-sensitive electrode after the addition of calcium (each 10 μM $CaCl_2$ pulse [arrows] was detected as a peak in calcium concentration). Three independent experiments gave similar results.

tion of DiOC6(3) uptake (increase in the% of DiOC6(3) low cells), occurred in a substantial proportion of DCs after 1 day of culture. This population had the same flow cytometric pattern of DCs treated with the protonophore mCICCP, a substance that abolishes $\Delta\psi$m that was used as a positive control (inset in Fig. 2C, left panel). The spontaneous loss of $\Delta\psi$m in cultured DCs was followed by enhanced ROS formation (at day 2) detected by the oxidation of HE to the fluorescent product ethidium (HE^+ cells) (Fig. 2C). Thus, mature DCs first disrupt their $\Delta\Psi$m and then hyper-produce ROS, the same sequence of events that has previously been observed in a variety of different models of cell death [27].

A double-staining procedure was developed to simultaneously assess DC $\Delta\Psi$m and cell viability (Fig. 2D) using the combination of DiOC6(3) and PI (Fig. 2D). All non-viable DCs (PI- marked DCs) had low $\Delta\psi$m (DiOC6(3) low), whereas viable DCs (PI-negative) contained two distinct subpopulations, one that exhibited a reduction in $\Delta\psi$m comparable with non-viable DCs and one that displayed high $\Delta\psi$m (Fig. 2D). Alternatively, the potentiometric fluorochrome CMX-ROS and the vital dye YOPRO-1 were used and gave the same result (not shown). These data indicate that the $\Delta\psi$m collapse occurs at an early stage of spontaneous DC death, before the loss of viability.

This double-staining procedure allowed us to sort the viable population of DCs in relation to their $\Delta\Psi$m. Thus, to univocally show that $\Delta\Psi$m low DCs indeed exhibit features of apoptosis, we purified viable (PI-negative) DC populations based on $\Delta\Psi$m in a fluorescence cell sorter followed by short-term culture. Low caspase-3/-7, -9 and -8 activities were found in DCs that still had a high $\Delta\psi$m, whereas DCs that had lost their $\Delta\psi$m showed significantly higher caspase-3/-7 and caspase-9 activities (Fig. 2E), demonstrating that apoptosis induction occurs predominantly in cells with a low $\Delta\psi$m. As previously reported [23], caspase-8 activity remained at low levels in both subpopulations of DCs. Moreover, when $\Delta\psi m^{high}$ and $\Delta\psi m^{low}$ fractions were stained with annexin V, we observed that almost all of the DCs sorted for $\Delta\psi m^{high}$ (>95%) were annexin V negative whereas many (75 +/– 10%) of the DCs sorted for $\Delta\psi m^{low}$ were Annexin V positive. These data, which confirm previous observations, indicate that $\Delta\psi_m$ low DCs are primed for spontaneous apoptosis.

To test whether mitochondrial dysfunction measured by $\Delta\psi$m reduction was also associated with perturbations in mitochondrial calcium homeostasis, we evaluated the calcium retention capacity of digitonin-permeabilized DCs with a calcium-sensitive electrode. The accumulation of calcium into mitochondria was assessed after repeated 10 μM $CaCl_2$ pulses until mitochondrial permeability transition (MPT) occurred and the accumulated calcium was released (Fig. 2F). After 2 days of culture (in comparison to day 0), DCs showed a markedly reduced mitochondrial ability to accumulate calcium and a decreased threshold level of calcium uptake, which is necessary for MPT to occur. Taken together, these data indicate that mitochondrial dysregulation appears at an early stage of constitutive DC apoptosis.

Regulation of constitutive DC death

To determine whether the caspase family of proteases is necessary for $\Delta\psi$m disruption and cell death, cells were incubated with z-VAD.fmk, a generalized irreversible caspase inhibitor. The z-VAD.fmk failed to prevent spontaneous $\Delta\psi$m disruption (Fig. 3A, left panel), confirming that caspases must act downstream of the mitochondrion. The z-VAD.fmk, at concentrations that completely block caspase activity, only delayed but did not prevent sponta-

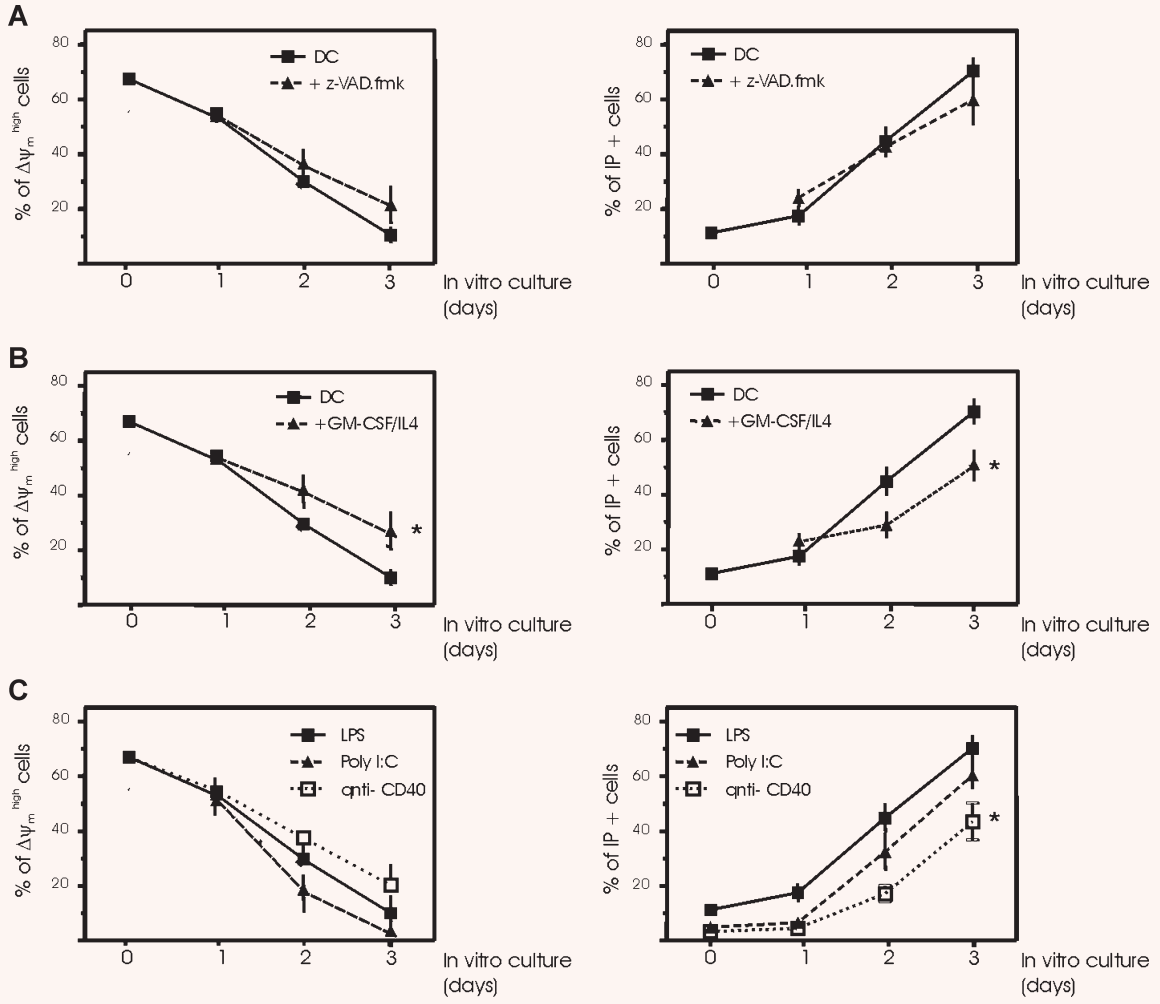

Fig. 3 Regulation of spontaneous DC death. Immediately after maturation, human monocyte-derived DCs were cultured for 4 days in the presence or absence of 100 μM z-VAD.fmk added every day (**A**) or culture medium supplemented every 2 days with 800 U/ml GMCSF and 100 U/ml IL-4 (**B**). Aliquots of cells were collected every day (0, 1, 2, 3 or 4 days of culture) for determination of Δψm (DiOC6(3) staining) and cell death (PI uptake). Mean ± S.D. from 5 independent experiments are shown. (**C**) Effects of maturation factors on spontaneous DC death. DCs were induced to mature by the addition of 1 μg/ml LPS for 18 hrs or 10 μg/ml poly (I:C) or 5 μg/ml anti-CD40 mAb and then mature DCs cultured for 4 days, with an aliquot of cells collected every day (0, 1, 2, 3 or 4 days of culture) for determination of Δψm (DiOC6(3) staining) and cell death (PI uptake). Mean ± S.D. from five independent experiments are shown.

neous DC death (Fig. 3A, right panel). We also asked whether the spontaneous reduction of ΔΨm and nuclear apoptosis could be reversed if a survival stimulus was applied (Fig. 3B). Thus, when the level of cytokines (GMCSF + IL-4) was maintained in the culture medium, Δψm disruption and DC death were significantly delayed during the first days of incubation, confirming the close association between the onset of death and mitochondrial dysfunction in DCs. However, this protective effect disappeared after 4 days of culture, even when cytokines were used at higher concentrations (data not shown).

To test the influence of maturation on spontaneous DC death, it was important to document the rate of death for different matu-

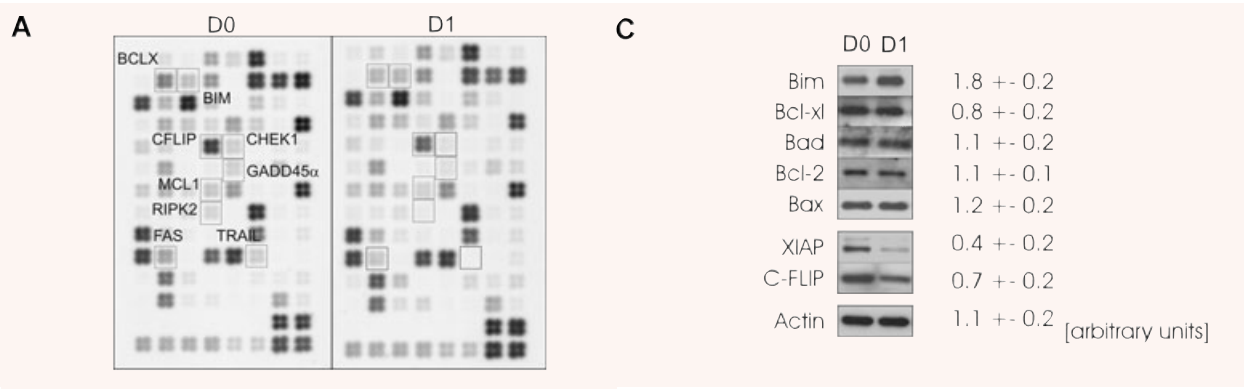

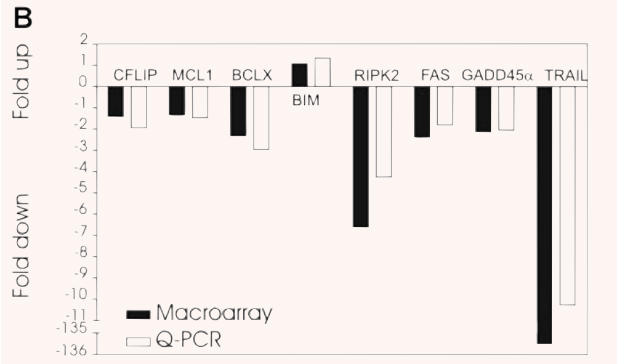

Fig. 4 Analysis of apoptosis-related gene expression during constitutive DC death. Apoptosis-related gene expression was analysed either immediately after maturation of human monocyte-derived DCs (day 0, D0) or at day 1 (D1) of standard culture (**A**). Gene expression changes were assessed by comparative filter cDNA macroarray measurements using a representative apoptosis array of mature DCs at day 0 and day 1 of culture as the example. One representative image of three independent experiments with separate donors is shown. (**B**) Expression changes of one up-regulated and seven down-regulated genes in DCs cultured for 24 hrs (D1) compared to DCs harvested immediately after maturation (D0). Similar changes were seen when DCs were compared *via* cDNA macroarray (black bars, $n = 3$) and quantitative (Q-PCR) (white bars, $n = 6$) (see Materials and Methods for details). (**C**) Analysis of DC apoptosis protein expression by Western blotting immediately after maturation (D0) or at day 1 (D1) of standard culture. The expression of several Bcl-2 members (Bim, Bcl-xl, Bad, Bcl-2, Bax) and the inhibitors of apoptosis, XIAP and c-FLIP, was analysed. Actin was used as a standard for equal loading of protein. One of four independent experiments with separate donors is represented. Four independent immunoblottings were scanned on a densitometer and the relative expression of proteins was determined. The intensity of the values obtained (mean ± S.E.M.) were expressed in arbitrary units.

ration agents stimulating DCs. Figure 3C illustrates that both $\Delta\Psi$m disruption and death occurred in poly (I:C)-stimulated DCs to an extent very similar to LPS-matured DCs. Conversely, maturation with agonistic antibodies to CD40 significantly reduced the occurrence of DC death after 3 days of culture, but was unable to prevent spontaneous mitochondrial dysfunction (Fig. 3C). As a consequence, it appears plausible that DCs characterized by a low $\Delta\psi$m are irreversibly programmed to die.

Changes in apoptotic gene expression profile during constitutive DC death

To gain new insights into the molecular processes that regulate mature DC apoptosis, we screened 96 apoptotic genes for changes in their expression profile. Using the apoptosis macroarray, we were able to identify 9 genes that were differentially expressed (1.5-fold difference) after 1 day in culture (Fig. 4A and B). Expression of genes encoding eight molecules diminished over 24 hrs in culture (Fig. 4), whereas we found that expression of the pro-apoptotic gene BIM was significantly increased (Fig. 4A and B). Real time quantitative-PCR supported the macroarray results for c-FLIP, Mcl-1, Bcl-X, Bim, Rip-2, Fas, Gadd45 and TRAIL, with minor differences only in scale of the down-regulation and up-regulation levels observed (Fig. 4B). On the basis of these results, the levels (relative to ß-actin) of some important apoptosis-related proteins were assayed by Western blot analysis. The anti-apoptotic proteins c-FLIP and XIAP were down-regulated in DCs at day 1 of culture compared with day 0 (Fig. 4C). It is known that the susceptibility of DCs to apoptotic signals is regulated, in part, by the relative levels and competing dimerizations between Bcl-2 family members [28]. After 1 day of DC culture, the pro-apoptotic protein, Bim, was also markedly increased, correlating with the mRNA profile; however, no change in other Bcl-2 family protein concentrations was evident (Fig. 4C). These data correlate well with the apoptotic phenotype determined in the previous experiments (Figs. 1–3). These results indicate spontaneous modulations in the expression of apoptosis-related genes in DCs likely accounts for facilitating spontaneous mitochondrial dysfunction and cell death to occur.

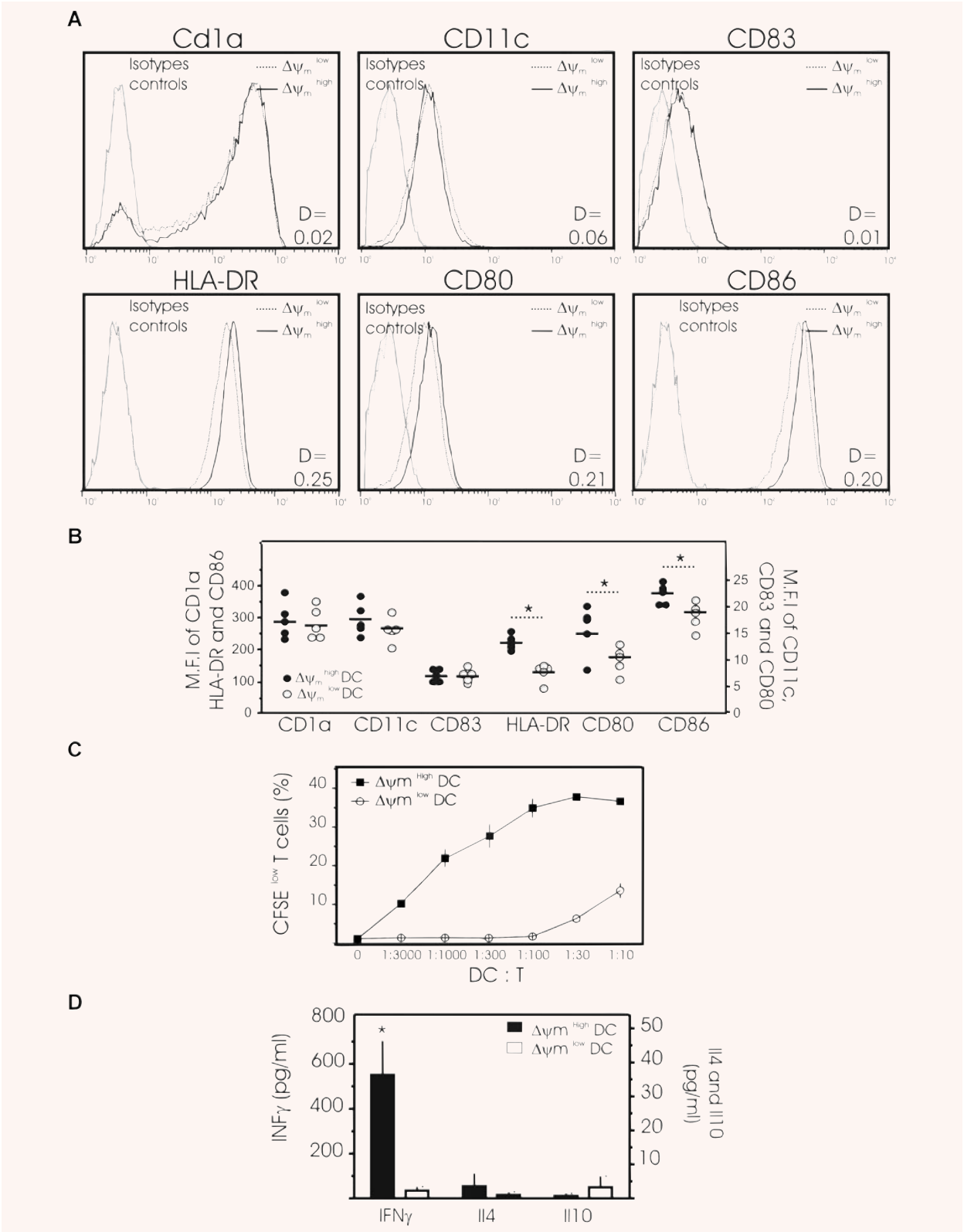

Fig. 5 Phenotypic and functional properties of DCs as a function of their $\Delta\psi$m. (**A**) Representative histograms showing the surface expression of CD1a, CD11c, CD83, HLA-DR, CD80 and CD86 on two subpopulations of mature DCs obtained from one donor: DCs with high $\Delta\psi$m (black line) and DCs with low $\Delta\psi$m (dotted line) (isotype controls = grey lines). Mature DCs were cultured for 48 hrs then harvested for the simultaneous determination of surface markers and $\Delta\psi$m using the potentiometric dye CMX-ROS. Dead cells and debris were gated out according to their forward-angle and right-angle light scattering properties. One of 4 independent experiments is presented. D values by Kolmogorov–Smirnov analysis between $\Delta\psi$m high and low subpopulations of DCs are shown. (**B**) Pooled data depicting the expression (MFI) of CD1a, CD11c, CD83, HLA-DR, CD80 and CD86 by $\Delta\psi$m high and low subpopulations of DCs as in (**A**) (Data are from five separate donors, circles represent single individuals and horizontal bars represent group mean values. $^*P < 0.05$ between the two groups). (**C, D**) Allo-stimulatory capacity of mature $\Delta\psi$m high and $\Delta\psi$m low DCs in activating allo-reactive T cells in an MLR assay. After 48 hrs of culture, mature DCs were stained with CMX-ROS and YOPRO and subpopulations of viable DCs with high $\Delta\psi$m and low $\Delta\psi$m sorted flow cytometrically. Then a graded number of $\Delta\psi$m high or $\Delta\psi$m low DCs were co-cultured with allogeneic, naïve $CD4^+$ T cells stained with CFSE. (**C**) After 5 days of co-culture, T-cell proliferation was determined by the percentage of CFSE low cells. The typical representation of proliferation curves determined at a different stimulator:responder ratio ranging from 1:3000 to 1:10 (DC:T) is shown. Three independent experiments gave similar results. (**D**) The secretion of IFNγ, IL4 and IL10 was measured by ELISA in the supernatants of T cells cultured for 5 days with viable $\Delta\psi$m high DCs (solid bar) or viable $\Delta\psi$m low DCs (open bar) sorted flow cytometrically (ratio 1 DC:10 T). Mean ± S.D. of three independent experiments with separate donors is shown. ($^*P < 0.05$ between the two subpopulations).

Correlation between $\Delta\Psi$m reduction and DC phenotypes and immuno-stimulatory functions

In a further series of experiments we attempted to correlate mitochondrial perturbations, as assessed by CMX-ROS staining, with the phenotye of mature DCs. Viable DCs were gated according to their forward/side scatter (FS/SS) properties. The combined assessment of antigenic phenotype and $\Delta\psi$m revealed that expression of the co-stimulatory molecules, *i.e.* HLA-DR, CD86 and CD80, was significantly different between high and low $\Delta\psi$m subpopulations of DCs (Fig. 5A and B). Although the $\Delta\psi$m low subpopulation did not display morphological signs of late apoptosis (*e.g.* cytoplasmic shrinkage), their expression of HLADR, CD80, and CD886 was significantly lower than that observed for $\Delta\psi$m high subpopulation of DCs (Fig. 5A and B). Conversely, both subpopulations of cells expressed similar levels of CD1a, CD11c and CD83, DC-specific markers, irrespective of their $\Delta\psi$m (Fig. 5A and B).

A more sophisticated approach was then used to corroborate these findings. Using the double-staining procedure described above, viable DCs were separated by cell sorting at day 2 of culture into two subpopulations, consisting of cells possessing either low or high $\Delta\psi$m. Each DC subpopulation purified with different $\Delta\psi$m values was then tested for their immuno-stimulatory functions (Fig. 5C and D). We first assessed the impact of $\Delta\psi$m on the capacity of mature monocyte-derived DCs to induce the proliferation of T cells in a mixed allogeneic leucocyte reaction (Fig. 5C). Therefore, $\Delta\psi$m high DCs or $\Delta\psi$m low DCs were co-cultured with allogeneic naive $CD4^+$ T cells for 5 days and the percentage of CFSE low T cells then estimated by flow cytometry. The $\Delta\psi$m low DCs were far less potent in inducing T-cell proliferation than $\Delta\psi$m high DCs (Fig. 5C). We next evaluated the capacity of both low and high $\Delta\psi$m DC subpopulations to induce T-cell cytokine production in a mixed allogeneic leucocyte reaction. $\Delta\psi$m low or $\Delta\psi$m high DC subpopulations were seeded with purified naïve $CD4^+$ $CD45RA^+$ T cells for 5 days, and the resultant culture supernatants analysed for production of IL-4, IL-10 and IFN-γ. Consistent with their inability to promote T-cell proliferation (Fig. 5C), the $\Delta\psi$m low DC subpopulation was unable to induce T-cell cytokine production (Fig. 5D). In contrast, the $\Delta\psi$m high DC subpopulation significantly induced secretion of the Th1 cytokine, IFNγ. Secretion of the Th2 cytokines IL4 and IL10 was not detected (Fig. 5D). As a consequence, the correlation between mitochondrial parameters and the activation of T cells appears to be coherent. Stimulated by these observations, we tested whether perturbations of mitochondrial function caused by rotenone, a specific inhibitor of mitochondrial respiratory chain complex I, might impair DC phenotype and immuno-stimulatory functions (Fig. 6). Incubation of DCs with rotenone for 4 hrs greatly reduced $\Delta\psi$m (Fig. 6A), decreased HLA-DR, CD80, and CD86 expression (Fig. 6B), and significantly reduced T-cell proliferation and IFNγ secretion (Fig. 6C). Overall, these results suggest that mitochondrial integrity is required for DC immune functions.

Discussion

Apoptosis represents the natural fate of end-stage differentiated cells including, presumably, monocyte-derived DCs. Apoptosis of DCs is probably a down-regulatory mechanism to halt excessive activation of the immune system. In this sense, splenic mouse DC trigger apoptosis soon after interaction with Ag-specific T cells [29]. The state of DC differentiation is a determining factor of their

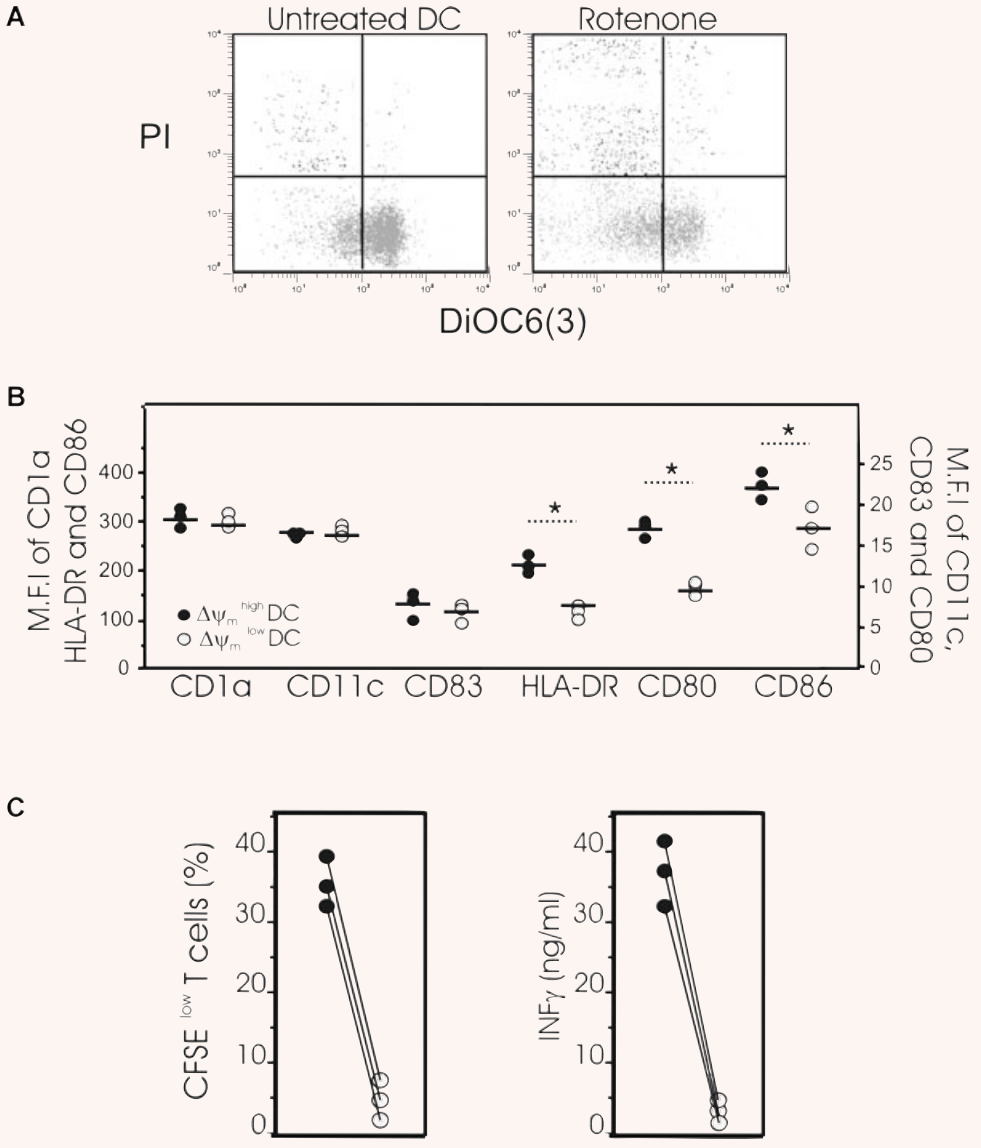

Fig. 6 Effects of rotenone on phenotypic and functional properties of DCs. (**A**) Mature DCs were incubated in the presence of 50 μM rotenone for 4 hrs or left untreated and then stained with DiOC6(3) and PI for simultaneous assessment of $\Delta\psi$m and viability. (**B**) Mature DCs incubated in the presence of 50 μM rotenone for 4 hrs were harvested for the simultaneous determination of surface markers (CD1a, CD11c, CD83, HLA-DR, CD80 or CD86) and $\Delta\psi$m using the potentiometric dye CMX-ROS. Dead cells and debris were gated out according to their forward-angle and right-angle scattering properties. Data are from three separate donors, circles represent single individuals and horizontal bars represent group mean values, $^*P < 0.05$ between the two groups. (**C**, left panel) Mature DCs were exposed to 50 μM rotenone for 4 hrs or left untreated then washed twice. Untreated DCs (●) or DCs exposed to rotenone (○) were co-cultured with allogeneic naïve $CD4^+$ T cells stained with CFSE. After 5 days of co-culture with DCs at a ratio 1:10 (DC:T), T-cell proliferation was determined by the percentage of CFSE low T cells present. The left panel represents data from three independent experiments. (**C**, right panel) The secretion of IFN-γ was measured by ELISA in the supernatant of T cells cultured for 5 days with DCs exposed to rotenone (●) or untreated DCs (○). Data represent three independent experiments.

susceptibility to apoptosis induced by diverse stimuli [7]. Pathogen- and T-cell-derived maturation confers resistance to environmental (*e.g.* treatment with glucocorticoids or UVB [12, 30]) and intrinsic death signals in DCs (such as Fas, TNFR1, and TRAIL [31]) by up-regulating anti-apoptotic factors [15, 32, 33]. Accordingly, we and others [10] found that spontaneous DC death, as measured by PI staining, was not important until after 3 days of culture. However, we observed the spontaneous appearance of closely associated changes including mitochondrial dysfunction, at early time points of incubation, when nuclear apoptosis was not yet evident. Thus, these mitochondrial changes appear to precede cell shrinkage, loss of plasma membrane viability and nuclear apoptosis, confirming previous similar findings for thymocytes and lymphocytes [34].

Bcl-2 family members regulate the lifespan of DCs [15]. We observed up-regulation of the pro-apoptotic BH3 protein of the Bcl-2 family, namely Bim, after 24 hrs of culture and no changes in the protein levels of any other Bcl-2 family members tested. Stimulation with LPS induced significant up-regulation of Bim, which is a crucial factor for spontaneous apoptosis in mice DCs [1]. Bim induces $\Delta\Psi$m loss and cytochrome c release in isolated mitochondria [35]. Thus, high correlations between Bim and death-inhibitory members of the Bcl-2 family may reflect an indication of commitment to death. Concomitantly, natural inhibitors of caspases, the proteins XIAP and c-FLIP, were down-regulated, suggesting that caspase activation requires the release of several physiological 'brakes' in DC apoptosis control. We observed a decrease in XIAP protein content in DCs without a significant change in XIAP mRNA levels, suggesting that XIAP degradation occurs in spontaneous DC death. The observed XIAP protein degradation is presumably dependent on the release of Smac/Diablo from mitochondria. This observation underlines the major role of mitochondria (and the mitochondrial Bcl-2 family of proteins) as the upstream regulator of spontaneous DC death. Interestingly, it has been demonstrated that, upon TLR engagement, an autocrine loop of IL-10 limited the longevity of DCs through the dynamic modulation of Bcl-2 protein expression, thus providing a rational explanation of mitochondrial involvement in DC death [36]. Environmental changes may also influence spontaneous DC death. Deprivation of growth factors causes mouse DCs to undergo apoptotic cell death within 48 hrs [33]. With monocyte-derived DCs from the same donor, the kinetics of apoptosis was delayed more than 24 hrs according to the batch of serum used for culture (not shown). Similar findings have been previously described with different batches of serum-free medium [37]. Nevertheless, in all cases, we observed exactly the same sequence of events, beginning with mitochondrial membrane changes.

With these facts in mind, we postulated that mitochondrial dysfunction represents a hitherto unrecognized mechanism for premature impairment of DC immune functions. We demonstrated an important correlation between mitochondrial dysfunction and the ability of DCs to activate naïve T cells. Although the exact causal relationship remains elusive, specific reduced expression of HLA and the co-stimulatory molecules CD80 and CD86 on $\Delta\Psi$m low DCs appears involved. It is noteworthy that when mature Langerhans cells spontaneously undergo apoptosis in culture, this process is also accompanied by reduced expression of various surface molecules, including CD86 [38]. Interestingly, it has been demonstrated that mitochondrial ROS are involved in the up-regulation of CD80 and CD86 in monocyte-derived DCs [39]. Balancing the mitochondrial membrane potential is important for ATP synthesis. Depolarization of mitochondrial transmembrane potential leads to disruption of respiratory chain function and ATP synthesis. It is generally assumed that cell proliferation and its associated metabolism are energy demanding processes, in contrast to the relatively low metabolic rate of quiescent cells, such as T lymphocytes, and probably also mature DCs. Nevertheless, the requirement of mitochondrial bioenergetics for DC differentiation, maturation and function warrant further investigation. Irrespective of these unknowns, the present results place a new emphasis on the putative role of mitochondria in the control of DC immune functions.

These results may also be of potential clinical relevance. Spontaneous apoptosis of DCs occurs *in vivo* and a higher percentage of apoptotic blood DCs is observed in patients with breast cancer compared to healthy volunteers [40]. In a unique experimental system employed to follow the migration and fate of DCs, DCs migrated into draining lymph nodes then disappeared rapidly (by 48 hrs) from the lymph nodes, probably by apoptosis [41]. The lifespan of antigen-bearing DCs has been estimated to be as short as 3 days [29, 42]. Thus, it is tempting to speculate that mitochondrial dysfunction in early DC apoptosis could be a plausible immune escape mechanism responsible for the failure of DC-based immunotherapy for cancer. Consequently, the assessment of mitochondrial membrane potential may allow for a direct estimation of pre-apoptotic DCs available for use and, thus, may provide a useful tool for the *in vitro*/*ex vivo* evaluation of DC-based vaccines before injection. The estimation of this mitochondrial parameter exposes a potentially significant subpopulation of pre-apoptotic DCs with impaired immuno-stimulatory capacities at a moment at which conventional tests addressing their viability fail to yield functionally positive results.

Acknowledgements

This work was supported by grants from the Ligue Contre le Cancer (Comité du Nord) (to PM), the Société Francaise de Dermatologie (to P.M.) and the Cancéropole Nord Ouest. A.S.H.-C. and L.C. received fellowships from the Cancéropole Nord Ouest and the Fondation de la Recherche Médicale, respectively. We thank N. Jouy (IFR 114) for her kind help.

References

1. **Chen M, Huang L, Wang J.** Deficiency of Bim in dendritic cells contributes to over-activation of lymphocytes and autoimmunity. *Blood.* 2007; 109: 4360–7.
2. **Josien R, Li HL, Ingulli E, *et al.*** TRANCE, a tumor necrosis factor family member, enhances the longevity and adjuvant properties of dendritic cells *in vivo*. *J Exp Med.* 2000; 191: 495–502.
3. **Wang J, Zheng L, Lobito A, *et al.*** Inherited human caspase 10 mutations underlie defective lymphocyte and dendritic cell apoptosis in autoimmune lymphoproliferative syndrome type II. *Cell.* 1999; 98: 47–58.
4. **Chen M, Wang YH, Wang Y, *et al.*** Dendritic cell apoptosis in the maintenance of immune tolerance. *Science.* 2006; 311: 1160–4.
5. **Willems F, Amraoui Z, Vanderheyde N, *et al.*** Expression of c-FLIP(L) and resistance to CD95-mediated apoptosis of monocyte-derived dendritic cells: inhibition by bisindolylmaleimide. *Blood.* 2000; 95: 3478–82.
6. **Marchetti P, Castedo M, Susin SA, *et al.*** Mitochondrial permeability transition is a central coordinating event of apoptosis. *J Exp Med.* 1996; 184: 1155–60.
7. **McLellan AD, Terbeck G, Mengling T, *et al.*** Differential susceptibility to CD95 (Apo-1/Fas) and MHC class II-induced apoptosis during murine dendritic cell development. *Cell Death Differ.* 2000; 7: 933–8.
8. **Jin H, Xiao C, Zhao G, Du X, *et al.*** Induction of immature dendritic cell apoptosis by foot and mouth disease virus is an integrin receptor mediated event before viral infection. *J Cell Biochem.* 2007; 102: 980–91.
9. **Nencioni A, Garuti A, Schwarzenberg K, *et al.*** Proteasome inhibitor-induced apoptosis in human monocyte-derived dendritic cells. *Eur J Immunol.* 2006; 36: 681–9.
10. **Vassiliou E, Sharma V, Jing H, *et al.*** Prostaglandin E2 promotes the survival of bone marrow-derived dendritic cells. *J Immunol.* 2004; 173: 6955–64.
11. **Sanchez-Sanchez N, Riol-Blanco L, de la Rosa G, *et al.*** Chemokine receptor CCR7 induces intracellular signaling that inhibits apoptosis of mature dendritic cells. *Blood.* 2004; 104: 619–25.
12. **Nicolo C, Tomassini B, Rippo MR, Testi R.** UVB-induced apoptosis of human dendritic cells: contribution by caspase-dependent and caspase-independent pathways. *Blood.* 2001; 97: 1803–8.
13. **Leverkus M, McLellan AD, Heldmann M, *et al.*** MHC class II-mediated apoptosis in dendritic cells: a role for membrane-associated and mitochondrial signaling pathways. *Int Immunol.* 2003; 15: 993–1006.
14. **Kriehuber E, Bauer W, Charbonnier AS, *et al.*** Balance between NF-{kappa}B and JNK(AP-1 activity controls dendritic cell life and death. *Blood.* 2005; 106: 175–83.
15. **Hou WS, Van Parijs L.** A Bcl-2-dependent molecular timer regulates the lifespan and immunogenicity of dendritic cells. *Nat Immunol.* 2004; 5: 583–9.
16. **Kim TW, Lee JH, He L, *et al.*** Modification of professional antigen-presenting cells with small interfering RNA *in vivo* to enhance cancer vaccine potency. *Cancer Res.* 2005; 65: 309–16.
17. **Peng S, Kim TW, Lee JH, *et al.*** Vaccination with dendritic cells transfected with BAK and BAX siRNA enhances antigen-specific immune responses by prolonging dendritic cell life. *Hum Gene Ther.* 2005; 16: 584–93.
18. **Hatzfeld-Charbonnier AS, Lasek A, Castera L, *et al.*** Influence of heat stress on human monocyte-derived dendritic cell functions with immunotherapeutic potential for antitumor vaccines. *J Leukoc Biol.* 2007; 81: 1179–87.
19. **Gallego MA, Joseph B, Hemstrom TH, *et al.*** Apoptosis-inducing factor determines the chemoresistance of non-small-cell lung carcinomas. *Oncogene.* 2004; 23: 6282–91.
20. **Marchetti P, Hirsch T, Zamzami N, *et al.*** Mitochondrial permeability transition triggers lymphocyte apoptosis. *J Immunol.* 1996; 157: 4830–6.
21. **Gallon F, Marchetti C, Jouy N, Marchetti P.** The functionality of mitochondria differentiates human spermatozoa with high and low fertilizing capability. *Fertil Steril.* 2006; 86:1526–30.
22. **Schmidt-Mende J, Gogvadze V, Hellstrom-Lindberg E, Zhivotovsky B.** Early mitochondrial alterations in ATRA-induced cell death. *Cell Death Differ.* 2006; 13: 119–28.
23. **Franchi L, Condo I, Tomassini B, *et al.*** A caspaselike activity is triggered by LPS and is required for survival of human dendritic cells. *Blood.* 2003; 102: 2910–5.
24. **van Gurp M, Festjens N, Van Loo G, *et al.*** Mitochondrial intermembrane proteins in cell death. *Biochem Biophys Res Commun.* 2003; 304: 487–97.
25. **Adrain C, Creagh EM, Martin SJ.** Apoptosis-associated release of Smac (DIABLO from mitochondria requires active caspases and is blocked by Bcl-2. *EMBO J.* 2001; 20: 6627–36.
26. **Zamzami N, Marchetti P, Castedo M, *et al.*** Sequential reduction of mitochondrial transmembrane potential and generation of reactive oxygen species in early programmed cell death. *J Exp Med.* 1995; 182: 367–77.
27. **Hirsch T, Susin SA, Marzo I, *et al.*** Mitochondrial permeability transition in apoptosis and necrosis. *Cell Biol Toxicol.* 1998; 14: 141–45.
28. **Pirtskhalaishvili G, Shurin GV, Gambotto A, *et al.*** Transduction of dendritic cells with Bcl-xL increases their resistance to prostate cancer-induced apoptosis and antitumor effect in mice. *J Immunol.* 2000; 165: 1956–64.
29. **Matsue H, Edelbaum D, Hartmann AC, *et al.*** Dendritic cells undergo rapid apoptosis *in vitro* during antigen-specific interaction with $CD4^+$ T cells. *J Immunol.* 1999; 162: 5287–98.
30. **Vizzardelli C, Pavelka N, Luchini A, *et al.*** Effects of dexamethazone on LPS-induced activation and migration of mouse dendritic cells revealed by a genome-wide transcriptional analysis. *Eur J Immunol.* 2006; 36: 1504–15.
31. **Leverkus M, Walczak H, McLellan A, *et al.*** Maturation of dendritic cells leads to up-regulation of cellular FLICE- inhibitory protein and concomitant down-regulation of death ligand- mediated apoptosis. *Blood.* 2000; 96: 2628–31.
32. **Miga AJ, Masters SR, Durell BG, *et al.*** Dendritic cell longevity and T cell persistence is controlled by CD154-CD40 interactions. *Eur J Immunol.* 2001; 31: 959–65.
33. **Rescigno M, Martino M, Sutherland CL, *et al.*** Dendritic cell survival and maturation are regulated by different signaling pathways. *J Exp Med.* 1998; 188: 2175– 80.
34. **Castedo M, Hirsch T, Susin SA, *et al.*** Sequential acquisition of mitochondrial and plasma membrane alterations during early lymphocyte apoptosis. *J Immunol.* 1996; 157: 512–21.

35. **Sugiyama T, Shimizu S, Matsuoka Y, *et al.*** Activation of mitochondrial voltage-dependent anion channel by a pro-apoptotic BH3-only protein Bim. *Oncogene.* 2002; 21: 4944–56.
36. **Chang WLW, Baumgarth N, Eberhardt MK, *et al.*** Exposure of myeloid dendritic cells to exogenous or endogenous IL-10 during maturation determines their longevity. *J Immunol.* 2007; 178: 7794–804.
37. **Royer PJ, Tanguy-Royer S, Ebstein F, *et al.*** Culture medium and protein supplementation in the generation and maturation of dendritic cells. *Scand J Immunol.* 2006; 63: 401–9.
38. **Ludewig B, Graf D, Gelderblom HR, *et al.*** Spontaneous apoptosis of dendritic cells is efficiently inhibited by TRAP (CD40-ligand) and TNF-alpha, but strongly enhanced by interleukin- 10. *Eur J Immunol.* 1995; 25: 1943–50.
39. **Yamada H, Arai T, Endo N, *et al.*** LPS-induced ROS generation and changes in glutathione level and their relation to the maturation of human monocyte-derived dendritic cells. *Life Sci.* 2006; 78: 926–33.
40. **Pinzon-Charry A, Maxwell T, McGuckin MA, *et al.*** Spontaneous apoptosis of blood dendritic cells in patients with breast cancer. *Breast Cancer Res.* 2005; 8: R5.
41. **Ingulli E, Mondino A, Khoruts A, Jenkins MK.** *In vivo* detection of dendritic cell antigen presentation to CD4+ T cells. *J Exp Med.* 1997; 185: 2133–41.
42. **Hermans IF, Ritchie DS, Yang J, *et al.*** CD8+ T cell-dependent elimination of dendritic cells *in vivo* limits the induction of antitumor immunity. *J Immunol.* 2000; 164: 3095–101.